

NANO EXPRESS

Open Access

Design of dual-diameter nanoholes for efficient solar-light harvesting

Cheng Zhang^{1,2}, Xiaofeng Li^{1,2*}, Aixue Shang^{1,2}, Shaolong Wu^{1,2}, Yaohui Zhan^{1,2} and Zhenhai Yang^{1,2}

Abstract

A dual-diameter nanohole (DNH) photovoltaic system is proposed, where a top (bottom) layer with large (small) nanoholes is used to improve the absorption for the short-wavelength (long-wavelength) solar incidence, leading to a broadband light absorption enhancement. Through three-dimensional finite-element simulation, the core device parameters, including the lattice constant, nanohole diameters, and nanohole depths, are engineered in order to realize the best light-matter coupling between nanostructured silicon and solar spectrum. The designed bare DNH system exhibits an outstanding absorption capability with a photocurrent density (under perfect internal quantum process) predicted to be 27.93 mA/cm², which is 17.39%, 26.17%, and over 100% higher than the best single-nanohole (SNH) system, SNH system with an identical Si volume, and equivalent planar configuration, respectively. Considering the fabrication feasibility, a modified DNH system with an anti-reflection coating and back silver reflector is examined by simulating both optical absorption and carrier transport in a coupled way in frequency and three-dimensional spatial domains, achieving a light-conversion efficiency of 13.72%.

Keywords: Photovoltaic device; Nanohole system; Light trapping; Light-conversion efficiency

PACS: 85.60.-q; Optoelectronic device; 84.60.Jt; Photovoltaic conversion

Background

Efficient light trapping plays a significant role in realizing high-performance photovoltaic devices [1-8], including nanophotonic crystals, metallic (plasmonic) nanostructures, and nanotextured surfaces. In recent years, directly nanopatterning the photoactive materials into arrays of nanowires (NWs) [9,10], nanoholes (NHs) [11,12], nanocones (NCs) [13], or nano-cone-holes (NCHs) [14] has also attracted intensive attention. Through unveiling the controllability of diameter and depth of NWs on the optical absorption, Hu and Chen proposed that NWs are good candidates for photovoltaics [9]. Lin and Povinelli demonstrated that NWs with a large lattice constant have an outstanding optical absorption arising from the increased field concentration and the excitation of guided resonant modes [10]. NHs were later investigated by Han

and Chen as an alternative light absorber that was proved to be superior to nanorod arrays [11].

Recently, Hua et al. investigated the absorption of multi-diameter nanopillars (MNPLs) systematically and showed that the absorption approaches that of NCs by increasing the number of nanopillar layers [15]. Furthermore, Fan et al. showed that dual-diameter NWs with a small-diameter tip and a large-diameter base exhibit an enhanced absorption over the wavelength range of 300 to 900 nm [16]. As NHs show superiority over NWs in light trapping, here, we study the possibility of further performance optimization of solar cells with NHs.

In this paper, through carefully examining the absorbing capability of NHs with different diameters, we propose the photovoltaic system composed of dual-diameter NHs (DNHs) with a large diameter at the top and a small diameter at the bottom, enabling broadband and strong optical absorption. The lattice constant, diameters, and depth ratio of the top and bottom NHs have been extensively studied in order to maximize the light absorption of the new system. The underlying physics have been explained by examining the absorption spectra as well as the spatial characteristics of the

* Correspondence: xfli@suda.edu.cn

¹College of Physics, Optoelectronics and Energy & Collaborative Innovation Center of Suzhou Nano Science and Technology, Soochow University, Suzhou 215006, China

²Key Lab of Advanced Optical Manufacturing Technologies of Jiangsu Province and Key Lab of Modern Optical Technologies of Education Ministry of China, Soochow University, Suzhou 215006, China

optical absorption. Our study indicates that the new stand-alone DNH system exhibits improved performance than previous single-diameter NHs (SNHs), NWs, and planar setups. Finally, the DNH design with the front anti-reflection coating and a back silver reflector is studied. Optoelectronic simulation allows us to evaluate the optical and electrical performance in a comprehensive way. It is predicted that the light-conversion efficiency can be up to 13.72%.

Methods

Figure 1 shows the schematic of the nanostructured photovoltaic system composed of (a) SNHs and (b) DNHs arranged in a square lattice (lattice constant a) with holes filled by air. The sunlight is incident on the system normally. The geometrical parameters have been inserted into the figure. The total hole depth (L for SNHs; $L_{\text{top}} + L_{\text{bot}}$ for DNHs) is fixed at 2.33 μm for a fair comparison with those of [9,11]. Based on the optical constants from Palik [17], simulations are performed by finite element method [18] with a maximum mesh size of 60, 28, and 40 nm for air, top silicon, and bottom silicon, respectively. With the calculated absorption spectrum, the maximum short circuit-current density under a perfect internal quantum process [11] is obtained by the

equation: $J_{\text{SC}} = \frac{e}{hc} \int_{310 \text{ nm}}^{\lambda_g} I(\lambda)A(\lambda)\lambda d\lambda$. The ultimate efficiency η which quantifies the overall absorption performance is given then by $\eta = \frac{\int_{310 \text{ nm}}^{\lambda_g} I(\lambda)A(\lambda) \frac{\lambda}{\lambda_g} d\lambda}{\int_{310 \text{ nm}}^{4,000 \text{ nm}} I(\lambda)d\lambda}$, where e

is the electron charge, h is the Planck constant, c is the light velocity in vacuum, $\lambda_g = 1,127 \text{ nm}$ is the wavelength corresponding to the bandgap energy of silicon, $I(\lambda)$ is the AM 1.5G standard solar irradiation spectrum [19], and $A(\lambda)$ is the absorptance. The spectral range is from

310 to 1,127 nm to characterize the light-matter coupling between silicon and solar incidence.

Keeping the fabrication feasibility in mind, an 80-nm ITO layer (working as the anti-reflection layer and contact) and a back silver reflector are introduced. The final photocurrent response of the new DNH solar cells through a detailed investigation on the internal carrier transport and recombination process is performed (see our previous publications [5,20-22]). The optoelectronic simulations include carrier generation, recombination, transport, and collection mechanisms with the carrier generation profile taken from the electromagnetic calculation. In this way, the actual external quantum efficiencies (EQEs) and the short-circuit photocurrent densities of the conventional SNH and the new DNH devices can be obtained. With the dark current response calculated [21] as well as the series and shunt resistances estimated from the experiment, the current-voltage (J - V) curve is achieved, allowing to evaluate the cell performances, such as open-circuit voltage (V_{oc}) and actual light-conversion efficiency.

Results and discussion

Figure 2a shows the dependence of the ultimate efficiency η on the lattice constant (a) and hole opening ratio (d/a). According to [14], the optimal lattice constant and filling ratio (f) of SNHs are about 600 nm and 0.5 (corresponding to $d/a = 0.8$), respectively, so d/a is limited from 0.7 to 0.9. For each d/a , η tends to rise and then drop with increasing a . The optimization occurs at $a = 600 \text{ nm}$ and $d = 480 \text{ nm}$, yielding $\eta = 26.17\%$, which is close to that reported in [14] (i.e., 26.52% when $a = 600 \text{ nm}$ and $f = 0.5$, i.e., $d/a = 0.8$).

Although with a high efficiency by SNHs, it is believed that the light-conversion capability of nanostructured photovoltaic system can be further improved with a proper modification of the device configuration. We therefore examine the absorption spectra of SNHs under two

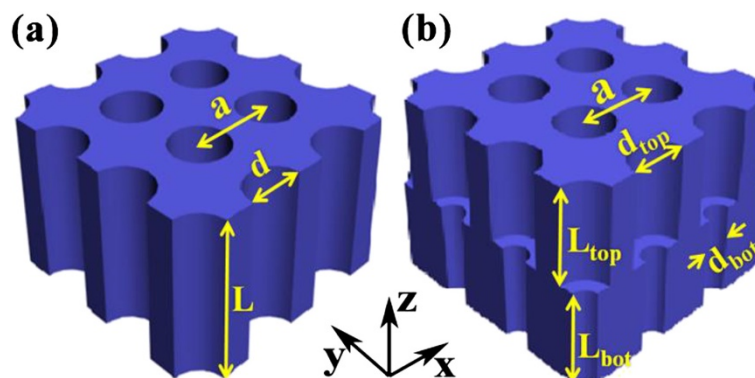
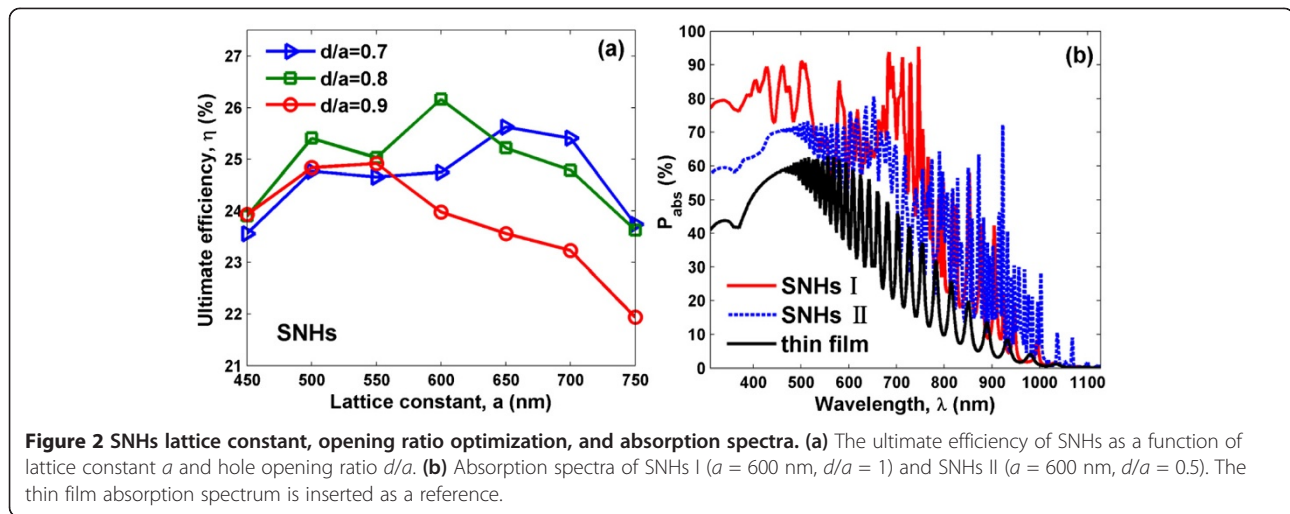


Figure 1 Device. (a) SNHs and (b) DNHs, where the geometrical parameters have been shown.



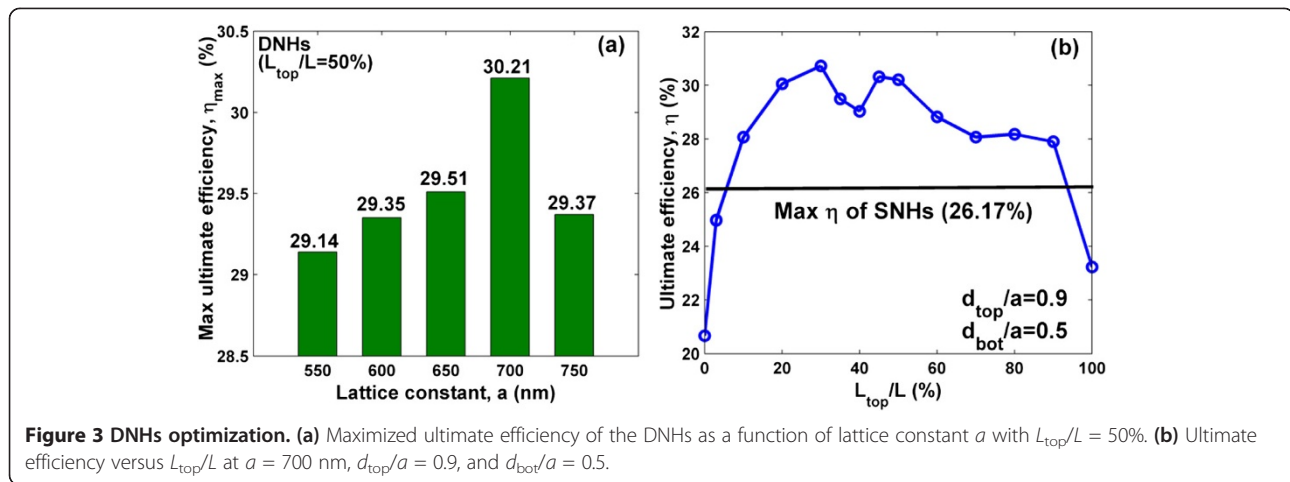
configurations, i.e., 1) large holes ($d/a = 1$) and 2) small holes ($d/a = 0.5$), as depicted in Figure 2b where the planar case (thickness = 2.33 μm) is also attached for comparison. It is observed that the absorption resonances exhibit obvious red shifts as d/a reduces [14]. This implies that SNHs with large holes show higher (weaker) light absorption in the short-wavelength (long-wavelength) region, while SNHs with smaller holes behave in a contrary way. The special diameter dependency can be interpreted by the fact that the effective refractive index of SNH system with large holes is relatively low (better impedance-matched with air), enabling more light entering the cell and greatly strengthening the light absorption in short-wavelength band [13]; nevertheless, the reduced active silicon material could not thoroughly absorb the long-wavelength light due to the much degraded material extinction coefficient [17].

The special relation between the spectral absorption behavior and physical size of NHs provides an effective way of managing and realizing a broadband optical absorption. Normally, short-wavelength (long-wavelength) light is absorbed by the region close to the top (bottom) facet. Therefore, we propose here a dual-layer nanostructured system (DNHs) which is composed by a top NH layer with large holes and a bottom NH layer with small holes. The dual-layer setup takes advantage of the super capability of NH systems with different hole sizes in absorbing solar incidence at specified spectral bands and thus contributes to a broadband enhancement.

We first examine the possibility of achieving a higher η from the dual-diameter NH photovoltaic system by properly engineering the lattice constants and hole diameters of both the top and bottom NH layers. In this study, it is assumed that two NH layers have an identical lattice constant, but the diameters (d_{top} and d_{bot}) can be artificially controlled in order to maximize η . The results

are listed in Figure 3a, where the highest η has been recorded for each a after a large number of three-dimensional optimizations by sweeping the top and bottom hole diameters (d_{top}/a from 0.7 to 1 and d_{bot}/a from 0.2 to 0.7). In addition, the hole depth ratio is temporarily fixed to be $L_{\text{top}}/L = 0.5$. It is found that the η of DNHs can be up to 30.21% when $a = 700$ nm, $d_{\text{top}}/a = 0.9$, and $d_{\text{bot}}/a = 0.5$. It is much higher than the best value of SNHs (26.17%) [14]. In fact, although with a high efficiency, the DNH system still leaves a room for further improvement by optimally setting the thickness ratio between the top and bottom NH layers. Figure 3b shows the tunability of η by adjusting L_{top}/L , which is considered to be from 0% (with only bottom NHs) to 100% (with only top NHs). The other parameters are borrowed from the design of Figure 3a. As displayed, the DNH system is usually better than SNH and shows the further increased $\eta = 30.72\%$ (i.e., $J_{\text{sc}} = 27.93$ mA/cm²) when $L_{\text{top}}/L = 30\%$, $a = 700$ nm, $d_{\text{top}}/a = 0.9$, and $d_{\text{bot}}/a = 0.5$. Actually, compared to the best SNHs (see the black line inserted in Figure 3b), there is a very wide range for L_{top}/L (i.e., 7% ~ 92%) to let the DNHs outperform the SNHs for solar applications.

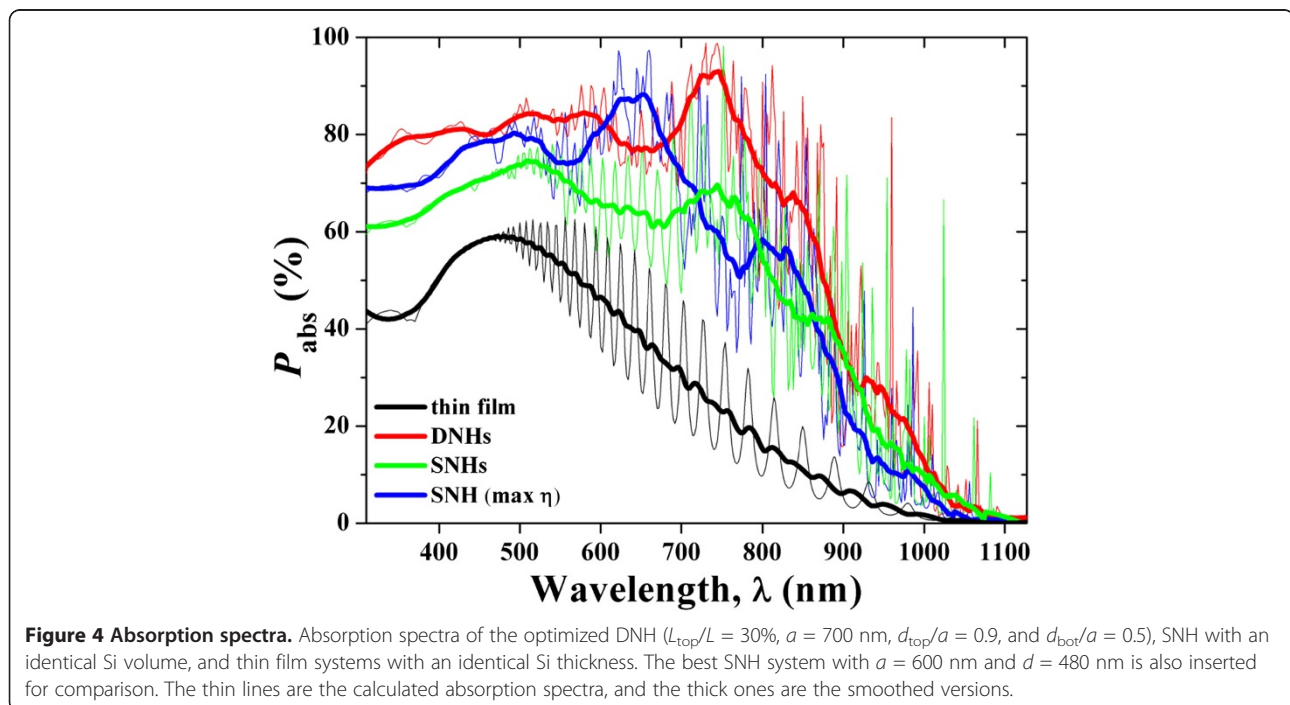
Figure 4 compares the spectral responses (absorption percentage (P_{abs})) of the photovoltaic systems under various nanoconfigurations (see figure caption for details). Although nanostructured photovoltaic systems show much improved ability of harvesting the solar incidence in the whole spectrum [11,12], DNHs exhibit the highest and most broadband absorption. Under the combined merits of large and small NHs, an ultra-broadband absorption enhancement is achieved except for a narrow band centered at around 650 nm, where the strong cavity resonances excited from the SNH system. The higher and broadband absorption enhancement results from the cavity resonant peaks excited in the DNH design. For



example, a distinct peak P_{abs} over 80% can be seen at the wavelength around 960 nm near λ_g , which is significantly higher than other cases, e.g., $P_{abs} = 27.77\%$ for the best SNHs. These results validate our initial consideration on the design of dual-diameter NHs and unveil the physics behind the absorption enhancement mechanisms. It is noted that if we compare the ultimate efficiency of the novel DNH system with the planar configuration under an identical Si thickness, the enhancement ratio of η is over 100%, as easily predicted from Figure 4.

It is now necessary to distinguish the absorption contributions from the top and bottom NH layers in order to thoroughly understand the optical response (see

Figure 5). It is shown that the majority of the incidence is absorbed by the bottom NH layer; however, the top NH layer dominates the absorption when $\lambda < 460$ nm as expected. Comparing the absorption spectra of the top and bottom NHs in long-wavelength region ($\lambda > 800$ nm), the bottom NH layer absorbs more light than the top, showing that the total DNH absorption peaks are actually mainly contributed from the bottom NH layer with small holes (in other words, larger Si volume). For an optical insight, the absorption coefficient of silicon to the long-wavelength light is very low, allowing the light to propagate into and being absorbed by the bottom NH layer. Moreover, the volume of the bottom small-NH layer is



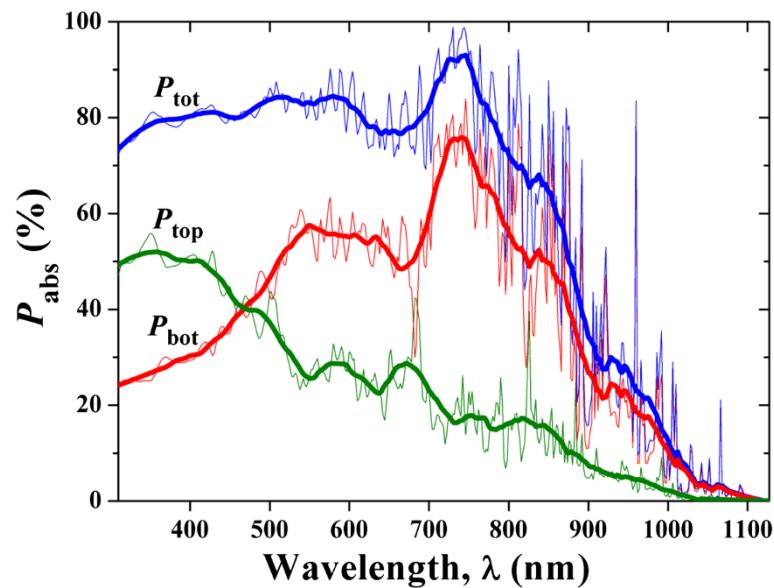


Figure 5 Absorption spectra. Absorption characteristics of the top/bottom nanoholes in the optimized DNHs. The absorption percentages of the total system, top NH layer, and bottom NH layer are defined here as P_{tot} , P_{top} , and P_{bot} , respectively. The thin lines are the calculated absorption spectra, and the thick ones are the smoothed versions.

larger than that of the top large-NH layer, which further improves the absorption of the bottom layer for the long-wavelength light. The absorption patterns at typical wavelengths (350, 700, and 960 nm) are shown in Figure 6. These patterns well illustrate the localized absorption inside the NH cavity and satisfactorily verify the previous observation and explanation. For example, under short-wavelength incidence, the light is mainly absorbed by the top NH layer and the region close to the hole (Figure 6a,b); under long-wavelength incidence, light penetrates into the Si volume and forms strong cavity resonant peaks. A distinct cavity effect can be seen from Figure 6e,f, where the strong Fabry-Perot resonant pattern is observed inside the bottom NH cavity, leading to the prominent peak around 960 nm as shown in Figure 4.

Finally, considering the realistic photovoltaic configurations, an ITO layer with a thickness of 80 nm, and a thin silver coating on the rear side are introduced into the optimal SNH and DNH systems (see Figure 7), to function as the contact, anti-reflection layer, and the back reflector, respectively. To evaluate the electrical response of the realistic devices, detailed simulations considering both optical absorption and carrier transport are performed [5,21]. The axial semiconductor junction is configured as follows: the donor (acceptor) concentration is 1.6×10^{20} (1×10^{18}) cm^{-3} , the n- and p-type regions are with an identical thickness of 150 nm, and the rest belongs to the intrinsic region. More parameters can be obtained from [23].

Figure 8 shows the P_{abs} and EQE spectra of the realistic SNH (a) and the newly designed DNH (b) systems.

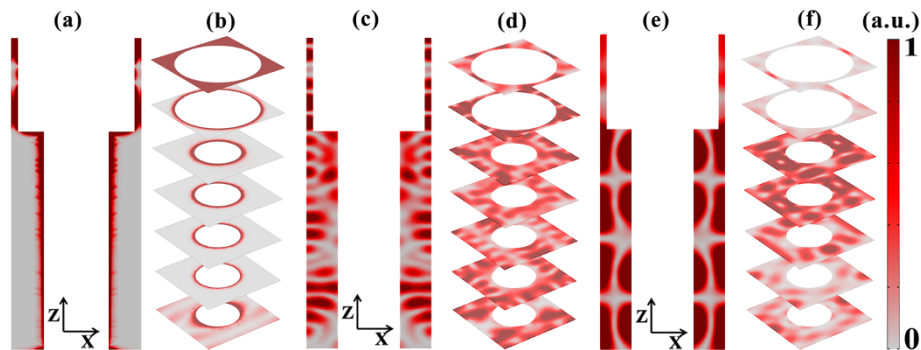


Figure 6 Optical absorption distributions. Spatial profiles of optical absorption in the optimized DNHs at $\lambda = 350$ nm (a, b), 700 nm (c, d), and 960 nm (e, f).

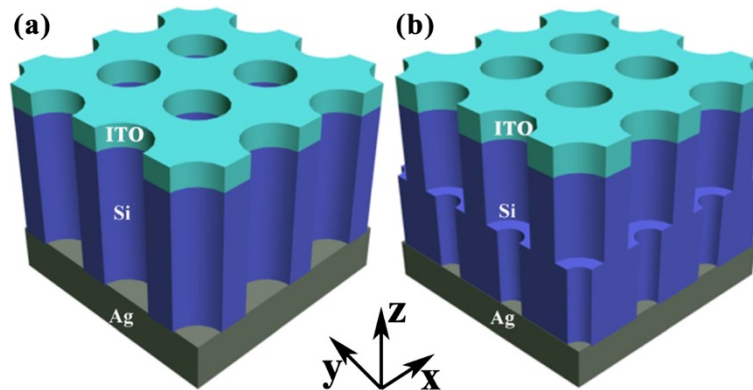


Figure 7 Realistic photovoltaic systems. SNH (a) and DNH (b) photovoltaic systems with an 80-nm front anti-reflection layer and a rear metallic reflector. The substrate is not shown in this figure.

Compared to P_{abs} in Figure 4, the absorptance in the short-wavelength range increased obviously due to the anti-reflection effect [3]. In addition, the light absorption in the long-wavelength range also increased on account of the re-absorption of the unabsorbed solar incidence in the first light path, which has been reflected back into the active region by the rear Ag reflector [1], although several narrow and strong absorption peaks in Figure 4

have disappeared in Figure 8b as the system configuration has been changed. The actual imperfect internal quantum process caused by the surface recombination and other carrier loss mechanisms results in a great degradation on the electrical properties of the device, implied as a big discrepancy between P_{abs} and EQE especially in the short-wavelength range. Through the spectral integration to the EQE spectra, J_{sc} of the realistic

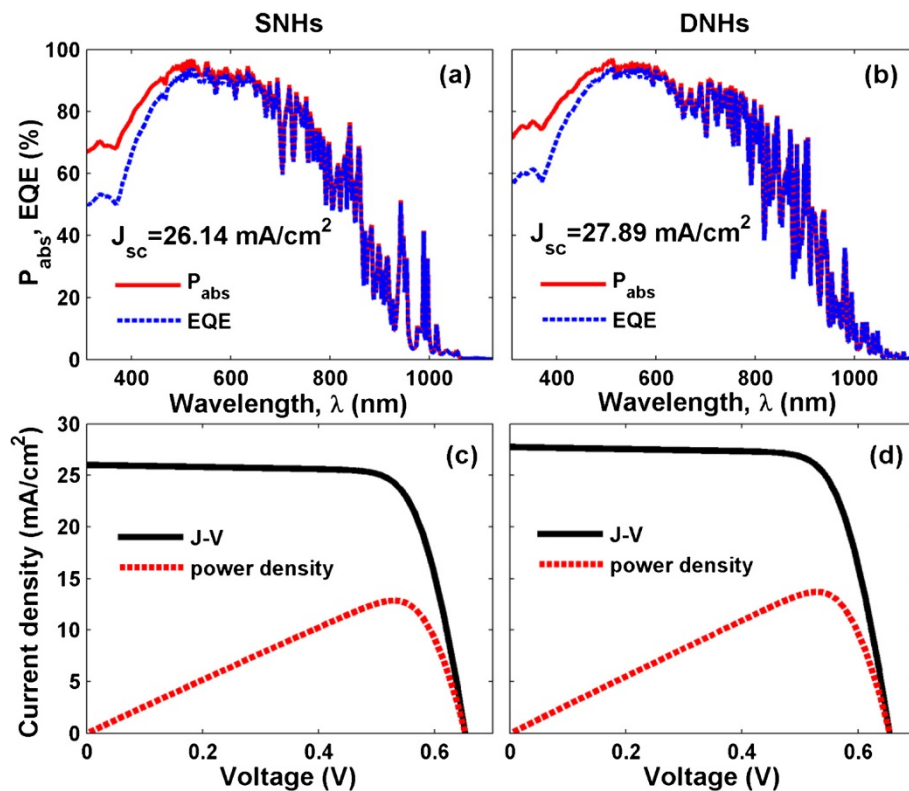


Figure 8 EQE spectra and J - V characteristics. The best SNH (a) and optimized DNH (b) photovoltaic systems with an 80-nm front anti-reflection layer and a rear metallic reflector. Corresponding J - V characteristics (c, d).

SNH and DNH devices are 26.14 and 27.89 mA/cm² (please note that the values directly converted from P_{abs} , i.e., without electrical simulation, are 27.06 and 28.66 mA/cm²), respectively.

The corresponding J - V characteristics are plotted in Figure 8c,d, based on the previously calculated J_{sc} and the dark current densities under continuously increasing forward electric bias (V). The series and shunt resistances (R_{s} and R_{sh}) can be roughly estimated by extracting the slope information from the J - V curve at the point of $V = 0$ and V_{oc} [24]. The values of R_{s} and R_{sh} are estimated to be around 2 and 1,000 Ω cm², respectively, by using the J - V curve from [25]. From the illustration, performance parameters like maximum output power density (P_{max}), V_{oc} , fill factor ($\text{FF} = P_{\text{max}}/(J_{\text{sc}}V_{\text{oc}})$), and the actual light-conversion efficiency can be obtained. It is found that J_{sc} is increased without degrading V_{oc} ($V_{\text{oc}} = 0.65$ V), leading to a higher P_{max} . Under a FF of approximately 76.01%, the light-conversion efficiency is predicted to be 13.72%. The actual efficiency is much less than the 'ultimate efficiency' from pure optical prediction since the carrier recombination and resistance losses are included.

Conclusions

We report the possibility of dramatically enhanced absorption of solar irradiance by using dual-diameter nanohole photovoltaic arrays. Broadband absorption enhancement is achieved by combining the merits of both small and large nanoholes which are spatially separated in different layers. Through a systematical optimization on the lattice constant, nanohole diameters, and depths of top and bottom NHs, the DNH photovoltaic system is designed to show a much improved ultimate efficiency up to 30.72% (i.e., $J_{\text{sc}} = 27.93$ mA/cm²), which is 17.39% (26.17%) higher than the best SNHs (SNHs with an identical Si volume). The novel DNH system shows light-absorbing capability which has doubled that based on conventional planar configuration. The better impedance match in the front surface and strengthened resonant cavity modes are responsible for the broadband enhancement in various wavelength regions. For a conventional realistic solar cell design, an 80-nm ITO layer and an Ag back reflector are included into the DNH system. Considering both optical and electrical perspectives, the realistic DNH device performs 13.72% light-conversion efficiency.

Abbreviations

DNH: dual-diameter nanohole; EQEs: external quantum efficiencies; FF: fill factor; J - V : current-voltage; MNPLs: multi-diameter nanopillars; NCs: nanocones; NCHs: nano-cone-holes; NHs: nanoholes; NWS: nanowires; P_{max} : maximum output power density; R_{s} : series resistances; R_{sh} : shunt resistances; SNH: single nanohole; V_{oc} : open-circuit voltage.

Competing interests

The authors declare that they have no competing interests.

Authors' contributions

CZ carried out the design and drafted the manuscript. XL conceived the design and supervised the research. AS and ZY participated in the J - V simulation. YZ and SW commented on the results and revised the manuscript. All authors read and approved the final manuscript.

Acknowledgements

This work is supported by the National Natural Science Foundation of China (Nos. 91233119, 61204066), Ph.D. Programs Foundation of Ministry of Education of China (No. 20133201110021), Graduate Education Innovation Project of Jiangsu Province of China (No. KYLX_1229), Natural Science Foundation of Jiangsu Province of China (Nos. BK20140349, BK20141200), China Postdoctoral Science Foundation (No. 2014M550301), '1000 Young Experts Plan' of China, and Priority Academic Program Development (PAPD) of Jiangsu Higher Education Institutions.

Received: 23 July 2014 Accepted: 7 September 2014

Published: 11 September 2014

References

1. Zeng L, Yi Y, Hong C, Liu J, Feng N, Duan X, Kimerling LC, Alamariu BA: Efficiency enhancement in Si solar cells by textured photonic crystal back reflector. *Appl Phys Lett* 2006, **89**:111111.
2. Mutitu JG, Shi S, Chen C, Creazzo T, Barnett A, Honsberg C, Prather DW: Thin film silicon solar cell design based on photonic crystal and diffractive grating structures. *Opt Express* 2008, **16**:15238–15248.
3. Li X, Zhang C, Yang Z, Shang A: Broadband, polarization-insensitive and wide-angle absorption enhancement of a-Si:H/ μ c-Si:H tandem solar cells by nanopatterning a-Si:H layer. *Opt Express* 2013, **21**:A677–A686.
4. Gomard G, Drouard E, Letartre X, Meng X, Kaminski A, Fave A, Lemiti M, Garcia-Caurel E, Seassal C: Two-dimensional photonic crystal for absorption enhancement in hydrogenated amorphous silicon thin film solar cells. *J Appl Phys* 2010, **108**:123102.
5. Li X, Hylton NP, Giannini V, Lee KH, Ekins-Daukes NJ, Maier SA: Bridging electromagnetic and carrier transport calculations for three-dimensional modelling of plasmonic solar cells. *Opt Express* 2011, **19**:A888–A896.
6. Yang Z, Shang A, Zhan Y, Zhang C, Li X: Ultra-broadband performance enhancement of thin-film amorphous silicon solar cells with conformal zigzag configuration. *Opt Lett* 2013, **38**:5071–5074.
7. Llopis F, Tobias I: The role of rear surface in thin silicon solar cells. *Sol Energ Mater Sol C* 2005, **87**:481–492.
8. Zhang C, Li X, Shang A, Zhan Y, Yang Z, Wu S: Performance-improved thin-film a-Si:H/ μ c-Si:H tandem solar cells by two-dimensionally nanopatterning photoactive layer. *Nanoscale Res Lett* 2014, **9**:73.
9. Hu L, Chen G: Analysis of optical absorption in silicon nanowire arrays for photovoltaic applications. *Nano Lett* 2007, **7**:3249–3252.
10. Lin C, Povinelli ML: Optical absorption enhancement in silicon nanowire arrays with a large lattice constant for photovoltaic applications. *Opt Express* 2009, **17**:19371–19381.
11. Han SE, Chen G: Optical absorption enhancement in silicon nanohole arrays for solar photovoltaics. *Nano Lett* 2010, **10**:1012–1015.
12. Leung SF, Yu M, Lin Q, Kwon K, Ching KL, Gu L, Yu K, Fan Z: Efficient photon capturing with ordered three-dimensional nanowell arrays. *Nano Lett* 2012, **12**:3682–3689.
13. Zhu J, Yu Z, Burkhard GF, Hsu CM, Connor ST, Xu Y, Wang Q, McGehee M, Fan S, Cui Y: Optical absorption enhancement in amorphous silicon nanowire and nanocone arrays. *Nano Lett* 2009, **9**:279–282.
14. Du QG, Kam CH, Demir HV, Yu HY, Sun XW: Enhanced optical absorption in nanopatterned silicon thin films with a nano-cone-hole structure for photovoltaic applications. *Opt Lett* 2011, **36**:1713–1715.
15. Hua B, Wang B, Yu M, Leu PW, Fan Z: Rational geometrical design of multi-diameter nanopillars for efficient light harvesting. *Nano Energy* 2013, **2**:951–957.
16. Fan Z, Kapadia R, Leu PW, Zhang X, Chueh YL, Takei K, Yu K, Jamshidi A, Rathore AA, Ruebusch DJ, Wu M, Javey A: Ordered arrays of dual-diameter nanopillars for maximized optical absorption. *Nano Lett* 2010, **10**:3823–3827.
17. Palik ED: *Handbook of Optical Constants of Solids*. Orlando: Academic; 1985.
18. Comsol Multiphysics. [http://www.comsol.com/].
19. ASTM: Reference solar spectral irradiance: Air Mass 1.5. [http://rredc.nrel.gov/solar/spectra/am1.5].

20. Li X, Zhan Y, Wang C: **Broadband enhancement of coaxial heterogeneous gallium arsenide single-nanowire solar cells.** *Prog Photovolt Res Appl* 2014, doi:10.1002/ppa.2480.
21. Li X, Hylton NP, Giannini V, Lee KH, Ekins-Daukes NJ, Maier SA: **Multi-dimensional modeling of solar cells with electromagnetic and carrier transport calculations.** *Prog Photovolt Res Appl* 2013, **21**:109–120.
22. Hylton NP, Li X, Giannini V, Lee K, Ekins-Daukes NJ, Loo J, Vercauteren D, Van Dorpe P, Sodabanlu H, Sugiyama M, Maier SA: **Loss mitigation in plasmonic solar cells: aluminum nanoparticles for broadband photocurrent enhancements in GaAs photodiodes.** *Sci Rep* 2013, **3**:2874.
23. Zhan Y, Li X, Li Y: **Numerical simulation of light-trapping and photoelectric conversion in single nanowire silicon solar cells.** *IEEE J Sel Top Quant Electron* 2013, **19**:4000208.
24. Nelson J: *The Physics of Solar Cells*. London: Imperial College Press; 2003.
25. Chen T, Yu P, Chen S, Chang F, Huang B, Cheng Y, Hsiao J, Li C, Wu Y: **Characteristics of large-scale nanohole arrays for thin-silicon photovoltaics.** *Prog Photovolt Res Appl* 2014, **22**:452–461.

doi:10.1186/1556-276X-9-481

Cite this article as: Zhang *et al.*: Design of dual-diameter nanoholes for efficient solar-light harvesting. *Nanoscale Research Letters* 2014 **9**:481.

Submit your manuscript to a SpringerOpen[®] journal and benefit from:

- ▶ Convenient online submission
- ▶ Rigorous peer review
- ▶ Immediate publication on acceptance
- ▶ Open access: articles freely available online
- ▶ High visibility within the field
- ▶ Retaining the copyright to your article

Submit your next manuscript at ▶ springeropen.com
